Tejinder Kaur, Arunachalam Thirugnanam* and Krishna Pramanik

Tailoring the *in vitro* characteristics of poly(vinyl alcohol)-nanohydroxyapatite composite scaffolds for bone tissue engineering

DOI 10.1515/polyeng-2015-0252 Received June 4, 2015; accepted October 5, 2015; previously published online February 27, 2016

Abstract: Poly(vinyl alcohol) reinforced with nanohydroxyapatite (PVA-nHA) composite scaffolds were developed by varying the nHA (1%, 2%, 3%, 4%, and 5%, w/v) composition in the PVA matrix by solvent casting technique. The developed composite scaffolds were characterized using scanning electron microscopy (SEM), X-ray powder diffraction (XRD), attenuated total reflectance-Fourier transform infrared (ATR-FTIR) spectroscopy, and contact angle measurement. The stability of the composite scaffolds in physiological environment was evaluated by swelling and degradation studies. Further, these composite scaffolds were tested for in vitro bioactivity, hemolysis, biocompatibility, and mechanical strength. SEM micrographs showed a homogenous distribution of nHA (3%, w/v) in the PVA matrix. XRD and ATR-FTIR analysis confirmed no phase contamination and the existence of the chemical bond between PVA-nHA at approximately 2474 cm⁻¹. PVA-nHA composite scaffolds with 3% (w/v) concentration of nHA showed nominal swelling and degradation behavior with good mechanical strength. The mechanical strength and degradation properties of the scaffold above 3% (w/v) of nHA was found to deteriorate, which is due to the agglomeration of nHA. The in vitro bioactivity and hemolysis studies showed improved apatite formation and hemocompatibility of the developed scaffolds. In vitro cell adhesion, proliferation, alkaline phosphatase activity, and Alizarin red S staining confirmed the biocompatibility of the composite scaffolds.

Keywords: biocompatibility; hemolysis; hydroxyapatite; mechanical strength; poly(vinyl alcohol).

1 Introduction

Natural bone is primarily composed of hydroxyapatite (HA) and collagen matrix. It has well-recognized functions such as providing mechanical support to the body, protection to internal organs, maintenance of calcium and phosphate homeostasis, and body movement [1]. Bone remodeling is a natural process by which old bone is continuously replaced by new bone tissue [2]. However, for few bone defects that do not heal naturally, surgical interventions are required. The nonavailability of donors and the risks associated with bone grafts imply the need for bone tissue engineering. The rapidly developing field of bone tissue engineering uses biodegradable and biocompatible scaffolds as three-dimensional supports for initial cell attachment. This in turn helps in the formation and growth of new tissues. Several key factors such as biocompatibility, biodegradability, pore size, and surface morphology have to be studied in detail for selecting an appropriate material for scaffold development [3]. The use of natural polymers as biomaterials and matrices or scaffolds for cell seeding is often limited by the poor mechanical performance and the loss of biological properties during its formulation [4]. On the contrary, synthetic polymers with relatively high mechanical strength can easily be molded into designed shapes, but their hydrophobic surface is not favorable for cell seeding [5]. To overcome these drawbacks, the development of composite scaffold becomes attractive, as it provides better mechanical and physiological demands of the host tissue.

Poly(vinyl alcohol) (PVA), a biodegradable and biocompatible polymer, has gained popularity as a scaffold material for tissue engineering because of its inherent nontoxicity, noncarcinogenicity, good biocompatibility, and desirable physical properties [6, 7]. However, PVA alone as a scaffold material has limitations, such as poor cell adhesion to tissues, owing to its bioinert nature and weak mechanical properties. Hence, the addition of an organic or inorganic additive to the PVA matrix will overcome these limitations and enhance its performance.

^{*}Corresponding author: Arunachalam Thirugnanam, National Institute of Technology, Department of Biotechnology and Medical Engineering, Rourkela, Odisha 769008, India, e-mail: thirugnanam.a@nitrkl.ac.in

Tejinder Kaur and Krishna Pramanik: National Institute of Technology, Department of Biotechnology and Medical Engineering, Rourkela, Odisha 769008, India

Among the bioactive inorganic materials, HA has gained widespread application because of its biocompatibility, bioactivity, osteoconductivity, and osteoproductivity [8]. HA, which mimics the stoichiometry of bone composition, easily bonds with the living bone tissue by forming a new apatite layer [9, 10]. However, owing to its poor mechanical properties, such as brittleness, low plasticity, and fatigue strength, HA is difficult to use as a monolithic in load-bearing applications [11]. To overcome these drawbacks, the combinations of monolithic [PVA and nanohydroxyapatite (nHA)] are used to improve the performance of the implants. It has been observed that PVA-HA composite exhibits improved physical and mechanical properties compared to pure PVA. Conversely, the homogeneous dispersion of nHA into the polymeric matrix is difficult to achieve in higher concentrations of nHA and leads to agglomeration due to high surface active energy. In previous studies, high concentrations of HA have been used, ignoring the fact that, above a certain percentage, HA starts agglomerating [12]. The agglomeration of nHA deteriorates the mechanical properties of the composites. Asran et al. [7] observed a decrement in tensile strength of PVA composite when reinforced with 10 wt% HA. This decrease in tensile strength was attributed to the agglomeration of HA at higher concentration. Additionally, the nHA concentration-dependent inhibition of osteoblast cells was also reported in literature. High calcium phosphate in the matrix was found toxic to osteoblast cells [13, 14]. Thus, the aim of this study was to overcome these problems by lowering the concentrations of nHA particles with optimized process parameters for achieving homogenous dispersion. In the present work, lower concentrations of nHA have been used to make scaffolds by solvent casting technique with improved mechanical and biological properties. The prepared scaffolds were characterized for in vitro biological properties (swelling, degradation, hemolysis, and bioactivity) and mechanical strength. The influence of nHA concentration on osteoblast cells was also evaluated by cell adhesion, cell viability and proliferation, alkaline phosphatase (ALP) activity, and Alizarin red S (ARS) stain-based assay.

2 Materials and methods

2.1 Preparation of PVA-nHA composite scaffolds

PVA (hot water soluble, HiMedia, average molecular weight 70,000-100,000, 98-100% hydrolyzed) and nHA (Acros Organics, particle size 50-70 nm) were used for composite development. Five different proportions of PVA-nHA composite scaffolds were synthesized using solvent casting method by dissolving 10% (w/v) of PVA in distilled water followed by the addition of nHA by varying its concentration (1%, 2%, 3%, 4%, and 5%, w/v). Homogenous dispersion was achieved by continuous stirring at 90°C, and the solution was poured into a glass mold and kept in a vacuum oven at 60°C for 24 h. The five resultant PVA-nHA composite scaffolds were designated as PHA 1, PHA 2, PHA 3, PHA 4, and PHA 5, respectively. These composites were characterized and their mechanical and in vitro biological properties were studied.

2.2 Characterization of PVA-nHA composite scaffolds

2.2.1 Scanning electron microscopy (SEM)

The surface morphology of the synthesized composite scaffolds was observed using SEM (JSM 6480LV, USA). The cross-sectional surfaces of the samples were analyzed using field emission-SEM (FESEM-FEI NovananoSEM 450). The scaffold samples were fixed via carbon tape and sputter coated with platinum before observing in SEM.

2.2.2 X-ray powder diffraction (XRD) analysis

XRD analysis was performed with a diffractometer (RigakuUltima IV diffractometer, Japan) to investigate the crystallinity and phase purity of PVA-nHA composite scaffolds. Diffraction data were collected from 15° to 60°, with a scan speed of 5°/min and step size of 0.05°. The crystallinity index (CI), as shown in Equation (1), was calculated using the height of (211) peak and minimum between (211) and (002) peaks, assuming that the intensity of (211) represents both crystalline and amorphous parts, whereas the minimum intensity at the mentioned location is for amorphous background. The CI from XRD provides qualitative and semiquantitative information about the amorphous and crystalline nature of the composite.

$$CI = (I_{211} - I_{am}) / I_{211}$$
 (1)

where I_{211} is the height of the (211) peak and I_{am} is the lowest height between the (211) and (002) peaks.

2.2.3 Attenuated total reflectance-Fourier transform infrared (ATR-FTIR) spectroscopy

ATR-FTIR (Thermo Scientific, Nicolet iS10, zinc selenide crystal) spectroscopy was performed to identify the functional groups present in the PVA-nHA composite scaffolds. The spectra were obtained over the scanning range of 550 to 4000 cm⁻¹.

2.2.4 Water contact angle measurement

Water contact angles were measured to evaluate the effect of nHA on the hydrophilicity of composite scaffolds. Water contact angles were measured by the sessile drop method at room temperature using a water contact angle analyzer (DSA 25, Kruss, Germany). Six static contact angle measurements were carried out after subtending water drops for 10 s on each scaffold. The average of six values is reported.

2.3 In vitro biological evaluation

2.3.1 Swelling studies

The extent of swelling of the PVA and PVA-nHA composite scaffolds was evaluated in phosphate-buffered saline (PBS) solution. Weighed dried samples were soaked in 10 ml PBS at 37°C. Then, the scaffolds were taken out at an interval of 1 h, surface dried, and reweighed. The swelling degree S_w (%) was calculated using Equation (2) [15]:

$$S_{w}$$
 (%)=[(W_{w} - W_{d} / W_{d})]×100 (2)

where W_w and W_d are the wet and dry sample weights, respectively.

2.3.2 Degradation studies

The in vitro biodegradation of the prepared PVA and PVA-nHA composite scaffolds was investigated by soaking them in simulated body fluid (SBF) solution for 6 weeks in a constant temperature water bath maintained at 37°C. The SBF solution was prepared as per the protocol suggested by Kokubo and Takadama [16]. All samples were kept in Falcon tubes and sealed with parafilm to minimize the change in pH and microorganism contamination. The SBF solution was not refreshed during the experiment. After soaking, the samples were filtered,

rinsed with distilled water, and dried at 40°C for 4 days, and the final weights were measured. The degradation percentage (D...) was calculated in the form of weight loss as in Equation (3) [17]:

$$D_{w} (\%) = [(W_{i} - W_{f}) / W_{i}] \times 100$$
 (3)

where W_i and W_i are the initial and final sample weights, respectively.

2.3.3 In vitro bioactivity studies

In vitro bioactivity was evaluated by examining the apatite formation on the PVA and PVA-nHA composites after soaking in SBF for up to 4 weeks. The samples were cut into dimensions of 1×1 cm² followed by soaking in SBF in a constant temperature water bath maintained at 37°C for up to 4 weeks. After soaking, the samples were taken out from SBF rinsed with distilled water, dried at 37°C for 12 h, and observed under SEM to evaluate the morphology of the apatite formed on the PVA-nHA composite scaffolds.

2.3.4 Hemolysis test

Samples of 1×1 cm² in dimension were cut and soaked in physiological saline (0.9%, w/v) for 24 h at 37°C. The samples were taken in tubes containing 10 ml physiological saline. Goat blood (20 ml) with potassium citrate solution (1 ml, 1 mg/ml) was diluted up to 4:5 (v/v) with physiological saline. Then, 0.5 ml of the diluted blood was added to each test tube and kept at 37°C for 1 h. For positive and negative controls, 0.5 ml blood was added to 10 ml distilled water and physiological saline, respectively. After 1 h, samples were centrifuged at 3500 rpm for 5 min, and its optical density (OD) was taken at 545 nm. The OD of the samples was measured in triplicate. The percentage of hemolysis was calculated according to Equation (4) [18]:

% Hemolysis=
$$[(OD_{test} - OD_{.ve})/(OD_{+ve} - OD_{.ve})] \times 100$$
 (4)

where OD, test, OD, and OD, are OD values of test, negative control, and positive control samples, respectively.

2.3.5 In vitro cell adhesion and morphology

The in vitro biocompatibility of the prepared PVA and PVA-nHA composite scaffolds was tested using human osteoblast-like MG 63 cell line (NCCS, Pune, India). Human osteoblast-like MG 63 cells were cultured in T-25 tissue culture flasks in a humidified atmosphere containing 5% CO₂ at 37°C. Dulbecco's modified Eagle's medium (Sigma-Aldrich, USA) supplemented with 10% fetal bovine serum and 100 U/ml penicillin-streptomycin was used. The scaffold samples were sterilized using UV treatment for 40 min before cell seeding. In brief, 1×10⁴ cells were seeded on the sterilized scaffolds into 24-well plate and incubated at 37°C in 5% CO₂ for 48 h. After incubation time, the samples were washed twice with PBS. Cells were then fixed with 2.5% glutaraldehyde solution for 3 h and dehydrated in a graded series of ethanol solution (30%, 50%, 70%, 90%, 95%, and 100%). The samples were vacuum dried, gold sputter coated, and observed using FESEM (FESEM-FEI NovananoSEM 450) to study the cell morphology and adhesion.

2.3.6 In vitro cell viability and proliferation studies

The cell viability and proliferation of human osteoblast-like MG 63 cells cultured on the prepared PVA and PVA-nHA composite scaffolds was evaluated using MTT assay. Osteoblast cells (1×104) were incubated on the scaffold samples in a 24-well plate at 37°C in 5% CO₂. After 48 h, 20 µl MTT (0.5 mg/ml) was added to each well, and cells were incubated for 4 h. Upon the removal of the MTT solution, the formazan crystals were solubilized in dimethyl sulfoxide by shaking the plate gently for 15 min. Absorbance was measured at 570 nm using UV-visible spectrophotometer (double-beam spectrometer 2203, Systronics, India). The performed tests in triplicates were compared with the control plate (24-well plate).

2.3.7 ALP activity

The ALP activity of MG 63 cells cultured on PVA and PVA-nHA composite scaffolds was analyzed using ALP colorimetric assay (Sigma-Aldrich, India). The scaffolds with cells were washed with PBS followed by the addition of lysis buffer. The p-nitrophenyl phosphate (pNPP) substrate was then added and the mixture was incubated for 1 h at 37°C. The reaction was stopped using 0.5 N NaOH, and the absorbance was measured at 405 nm using UV-visible spectrophotometer. The cell culture plate, seeded with cells, was taken as the control. Three replicates of scaffold samples were used from each group.

2.3.8 Mineralization assay

Calcium deposition due to matrix mineralization on the PVA-nHA composite scaffolds was quantified using ARS stain-based colorimetric assay. The scaffold samples with cells were washed with PBS and fixed with 70% ethanol for 1 h at 4°C. These samples were washed thrice with distilled water and then stained with ARS stain for 30 min. After a series of distilled water washes, the stain was eluted with 10% cetylpyridinium chloride and incubated for 30 min. The absorbance of the eluted dye was measured at 562 nm using a spectrophotometer. The cell culture plate, seeded with cells, was taken as the control. A calibration curve was also plotted for known concentrations of ARS. Three replicates of scaffold samples were used from each group.

2.4 Tensile strength measurement

The tensile strength of the developed composite scaffolds was carried out on a universal testing machine (ElectroPuls E1000, Instron, UK) as per ASTM D3039 [19]. A load cell of 250 N was used, a strain rate of 2 mm/min was applied, and measurements were taken. Testing was carried out in triplicate. The cross-section of the fracture surface of sample PHA 4 and PHA 5 was also examined by using FESEM (FESEM-FEI NovananoSEM 450).

3 Results and discussion

3.1 SEM analysis

The morphology of the composite scaffold that depends on the composition of the scaffold material plays a major role in the durability and performances of the composites as well as on cell adhesion and growth. The agglomeration of nHA in the polymer matrix might affect properties such as swelling, degradation, mechanical strength, and protein adsorption. The homogeneous dispersion of nHA in the PVA matrix aids in the improvement of the physical, mechanical, and biological properties of the composite. Microstructural analysis was done on all composite scaffolds to analyze whether the homogeneous dispersion of nHA in the PVA matrix has been achieved, which is followed by apatite formation in the matrix. SEM micrographs of different scaffold samples are shown in Figure 1. SEM micrographs have revealed the distribution of nHA in the PVA matrix, which plays a major role in the surface roughness of these composites as the concentration of

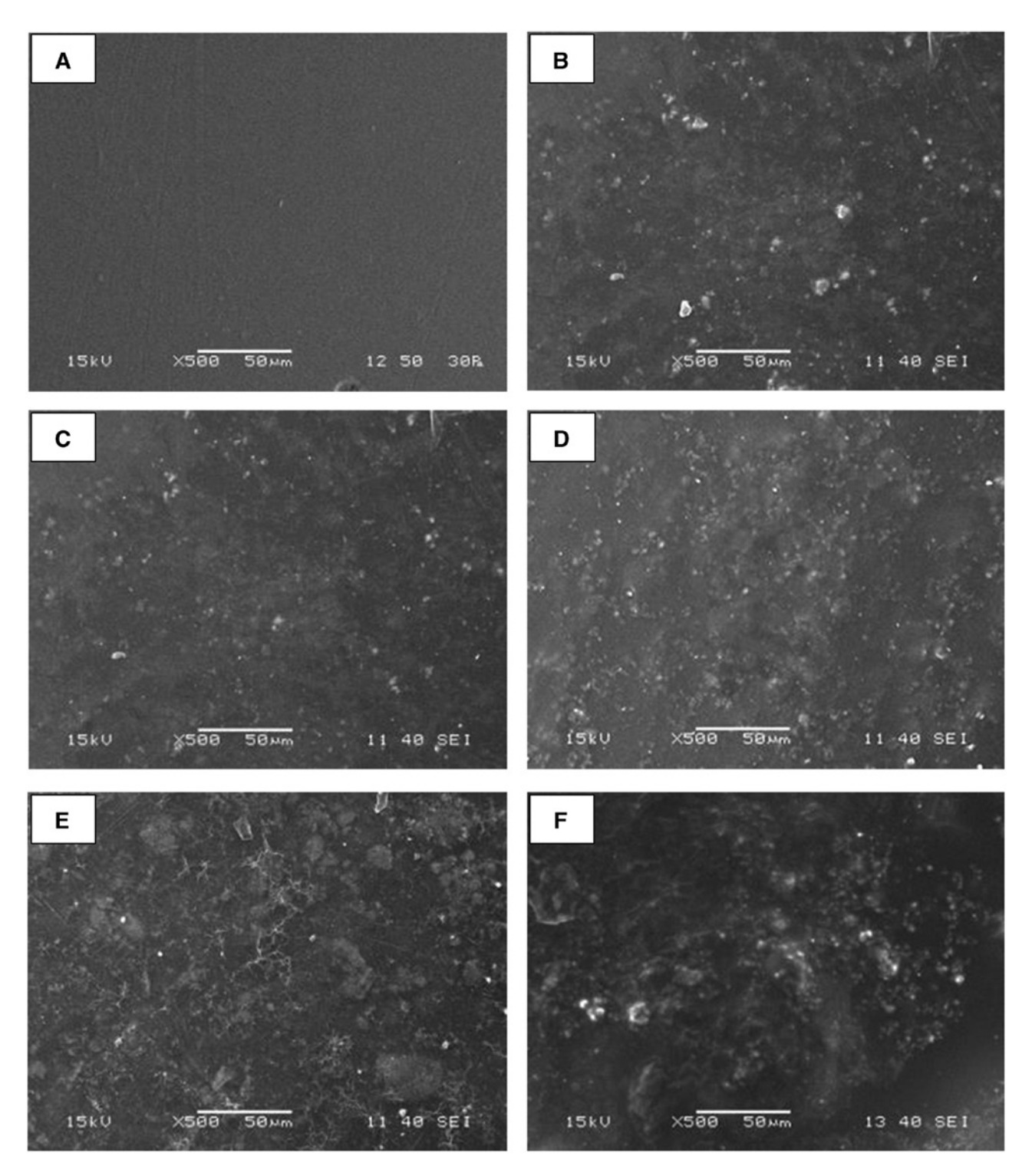


Figure 1: SEM micrographs of PVA and various PVA-nHA composites: (A) PVA, (B) PHA 1, (C) PHA 2, (D) PHA 3, (E) PHA 4, (F) PHA 5.

nHA has been varied from 1% to 5% (w/v). The micrograph of PVA scaffold without nHA (Figure 1A) shows a smooth surface, owing to the bioinert nature of PVA. The micrographs (Figure 1B-F) show that, with the addition of nHA in the PVA matrix, surface roughness has been increased. PHA 1 and PHA 2 samples have shown a homogeneous dispersion of uniformly sized clusters of nHA particles. With a further increase in the concentration of nHA particles, the roughness was found to increase as in PHA 3. The microstructural analysis also reveals that the agglomeration of nHA in the PVA matrix increases with the increase in the concentration of nHA. PHA 3 shows some regions of agglomerated nHA particles, with 3% (w/v) of nHA as in Figure 1D. In the microstructure of composite scaffolds, PHA 4 and PHA 5, more agglomerated clusters were observed as in Figure 1E and F. Similar results were also observed and reported by Yusong et al. [20]. The formation of agglomerated nHA clusters might be attributed to the charged inorganic ions that were not evenly distributed in the PVA matrix, thereby getting agglomerated clusters under the effect of van der Waals force and Brownian motion. Brownian motion causes the collision of the nHA particles with each other and the van der Waals forces attract these particles leading to agglomeration. From the SEM micrographs, with the increase in the concentration of nHA above a certain amount (3%, w/v), more agglomeration was evident, which could affect the mechanical and biological properties of composites.

3.2 XRD analysis

The XRD spectra of PVA and PVA-nHA composite scaffolds with different nHA concentrations (Figure 2) were obtained to investigate the formation of any new phase or contamination during processing. The broad diffused peak at 19.5° corresponding to the characteristic peak of PVA (Figure 2) demonstrates that PVA possesses a semicrystalline structure that was observed in all composite scaffolds. No other peaks were found in the PVA sample, indicating that there is no phase contamination. The HA characteristic peaks

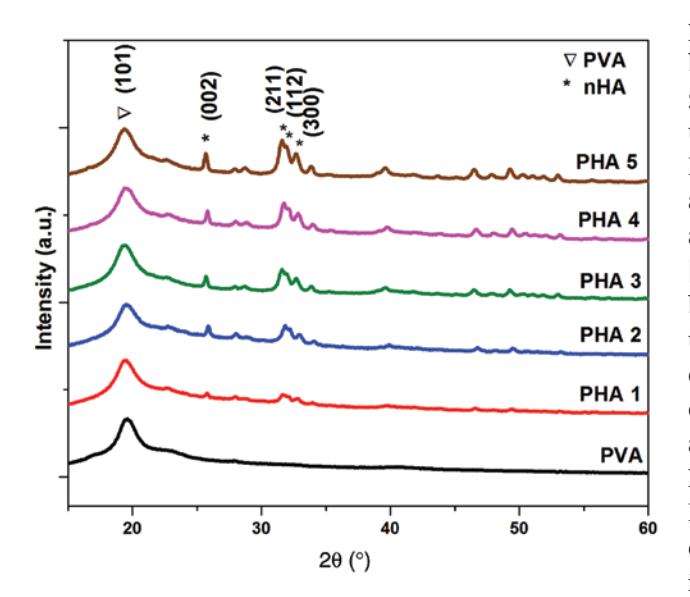


Figure 2: XRD pattern of the processed PVA-nHA composites.

Table 1: CIs of composite samples.

Samples	CI (%)
PHA 1	21.4
PHA 2	30.0
PHA 3	40.4
PHA 4	41.0
PHA 5	46.2

at 25.87°, 31.77°, and 32.90° were observed for all sample compositions containing nHA and confirmed with the JCPDS standard for HA (PDF No. 09-0432) [21]. The intensity of HA peaks was found to increase from PHA 1 to PHA 5 samples as nHA concentration increases. No intermediate calcium phosphate phases such as tricalcium phosphate or biphasic calcium phosphate were observed in all processed PHA composite scaffolds. The CIs for the composite samples calculated from the XRD pattern (Figure 2) are listed in Table 1. The CI was found to increase from 21.48% (PHA 1) to 46.2% (PHA 5) with the increase in nHA concentration. This infers that the crystallinity increases as the concentration of nHA increases from 1% to 5% (w/v) of nHA in the PVA matrix.

3.3 ATR-FTIR analysis

The ATR-FTIR analysis of the as-developed composite scaffolds was done to study the changes in the chemical bonding of nHA with PVA during processing. The FTIR spectra of PVA-nHA composite scaffolds are shown in Figure 3. The spectra show the characteristic peaks corresponding to standard PVA and nHA. PVA is a polar polymer having -CH, -CH,, and -OH side groups with C-C backbone. On the C-C backbone, PVA has -OH pendant groups that make PVA capable of physical crosslinking. All these characteristic functional groups were observed in the FTIR spectra of PVA. A broad absorption band obtained at approximately 3500 and 3000 cm⁻¹ corresponds to the interaction of absorbed -OH group present in both nHA and PVA [22]. The bonding between PVA and nHA became stronger because of the increase in the number of -OH groups with the addition of nHA in PVA. This is due to the attraction of Ca⁺ ions onto the -OH group of PVA. The peak at 2920 cm⁻¹ indicates the stretching of -CH₂. The weak absorbance at approximately 2474 cm⁻¹ represents the interaction of hydrogen atoms of PVA with phosphorous atoms of nHA. Poursamar et al. [11] also obtained a similar peak at 2430 cm⁻¹, indicating PVA and nHA interactions. The difference in the concentration of nHA added might be the reason for the peak shift of ~40 cm⁻¹. The absorption band associated

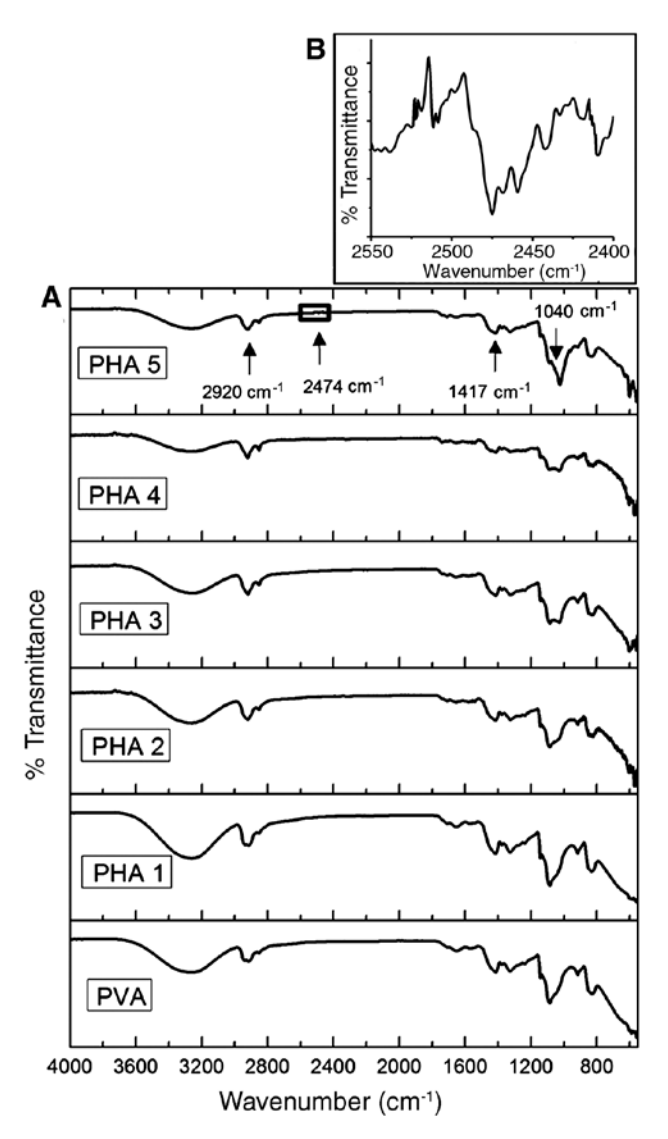


Figure 3: ATR-FTIR spectra of (A) PVA-nHA composites and (B) peak at 2474 cm-1 in PHA 5.

with the stretching of H₂O molecules was observed at 1640 cm⁻¹. Peaks with low intensity observed at approximately 1470 cm⁻¹ correspond to the stretching vibration of -CO₂² ions due to atmospheric -CO₂ absorption. The absorption at approximately 1417 cm⁻¹ originates from C-H bend and C-C stretching. The intensity of this peak was found to decrease with the increase in the concentration of nHA. The peak for C-O stretching was observed at approximately 1083 cm⁻¹. The characteristic peaks for stretching vibration of phosphate ion (PO, 3-) at 1040 cm-1 were observed at the higher concentration of nHA. This peak was absent in pure PVA scaffold. Other characteristic peaks for nHA were present at 960 cm⁻¹ (symmetric P-O), 560 cm⁻¹, 570 cm⁻¹, and 601 cm⁻¹ (O-P-O bend) [23]. The intensity of these bands was very low because of the less concentration of nHA used in processing from 1% to 5% (w/v).

Table 2: Average contact angles of PVA-nHA composites.

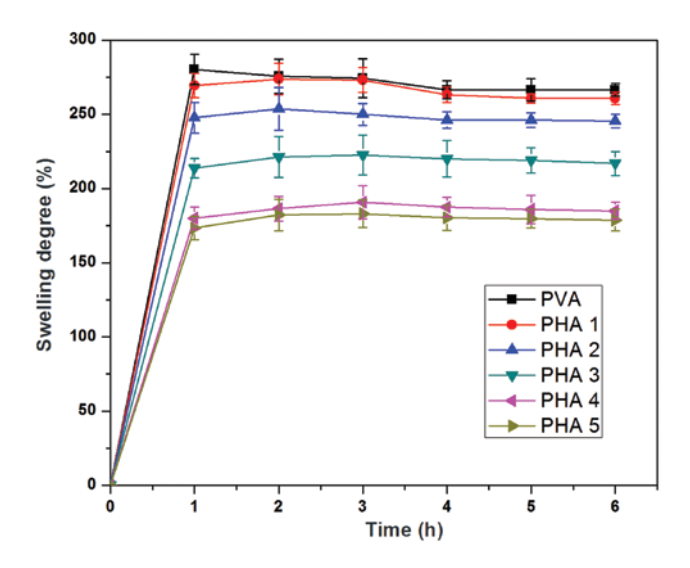
Samples	Average contact angle (°)
PVA	40.2
PHA 1	50.4
PHA 2	51.8
PHA 3	60.7
PHA 4	67.3
PHA 5	71.5

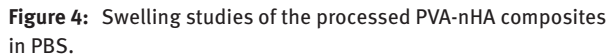
3.4 Water contact angle measurement

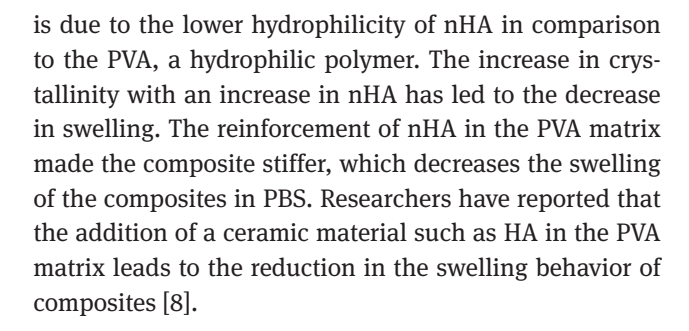
The water contact angles of PVA and PVA-nHA composite scaffolds are shown in Table 2. The contact angles of all composites were found to be <80°, indicating the hydrophilic behavior of the scaffolds. Pure PVA without nHA showed the lowest contact angle of 40.2°. The contact angles of PVA-nHA composites gradually increased with the increasing concentration of nHA. The increase in contact angles and the decrease in the hydrophilicity of the composite scaffolds correspond to the addition of hydrophobic nHA. Chau et al. [24] have reported that the contact angle depends not only on surface roughness but also on surface chemistry and hydrodynamic conditions. In the case of hydrophilic surfaces, contact angle decreases with the increase in surface roughness. However, in the present study, contact angle was found to increase with the increase in roughness due to the addition of nHA. The hydrophilic nature indicates the suitability of these scaffolds for cell adhesion and growth.

3.5 Swelling studies

The swelling behavior of a scaffold is a prime factor for tissue engineering application. The degree of swelling of the composite scaffold is dependent on their composition and hydrophilic nature. The influence of the concentration of the nHA in composites on their swelling behavior in PBS is shown in Figure 4. The reinforcement of nHA in the PVA matrix brings about a significant change in the swelling behavior of these composite scaffolds. Results have indicated that swelling degree curves of PVA-nHA composite increase with immersion time and get saturated after 1 h. PVA without nHA showed the highest degree of swelling equal to 280% after 1 h of soaking in PBS. The degree of swelling for other scaffolds is as follows: 269% (PHA 1), 247% (PHA 2), 213% (PHA 3), 180% (PHA 4), and 173% (PHA 5). With the increase in the concentration of nHA, the degree of swelling was found to decrease, which







3.6 Degradation studies

Biodegradability is an essential factor that has to be considered while developing a composite scaffold. The degradation rate influences the mechanical properties and inflammatory responses of the scaffold. It has been reported that biodegradable polymers provoke more intense inflammatory responses compared to nondegradable polymers [25]. Further degradation is influenced by many other factors such as molecular weight, chemical structure, presence of reinforcement, and its dispersion. SBF was used as a degradation medium in this study. Figure 5 shows the weight loss of the developed PVA-nHA composites of different nHA concentrations soaked in the SBF solution at 37°C. The PVA scaffold without the addition of nHA shows more weight loss. With the addition of nHA, weight loss was found to decrease due to the decrease in porosity in the PVA matrix with the increase in nHA concentration. In the pure PVA scaffold, voids were reported through which SBF must have diffused and degraded the matrix [20].

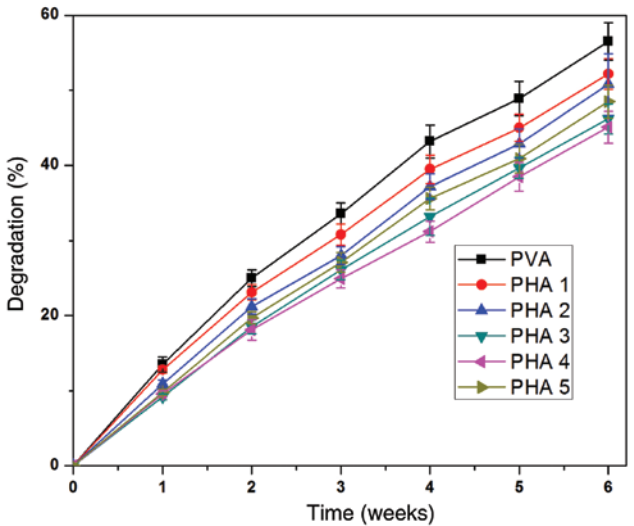


Figure 5: Degradation studies of the processed PVA-nHA composites in SBF.

Immersion of the scaffolds in SBF caused it to swell, breaking the weaker bonds in the composite. The addition of nHA makes the structure of scaffold denser, making it more difficult to dissolute. The scaffolds with higher nHA have lower swelling degree attributed to its hydrophobic behavior, and the particles itself cannot swell. Hence, the less SBF uptake in composite scaffolds resulted in slower degradation compared to PVA alone. The degradation results can also be correlated with XRD data (Section 3.2). Researchers have reported that, with the increase in the crystallinity of the material, the degradation rate decreases [10]. From the XRD spectra, an increase in CI was observed (Table 1) with the increase in the concentration of nHA, indicating slower degradation rate. On the contrary, the composite scaffold PHA 5 shows a higher degradation rate than PHA 3 and PHA 4. This might be due to more agglomeration and improper dispersion of nHA in addition to the voids in the PVA matrix. Due to this, SBF must have penetrated the matrix more easily and breaking the bond between the agglomerated nHA and degrading the matrix in PHA 5, owing to higher degradation compared to PHA 4 and PHA 3. Among all composite scaffolds, PHA 3 shows a nominal degradation rate due to the uniform distribution of nHA in the PVA matrix, thereby filling up the voids and increasing the hydrophobic nature of the composite.

3.7 In vitro bioactivity studies

Bioactivity is the ability of the material to bond with the host bone tissue. HA is widely used for bone tissue engineering because of its high bioactive properties matching that of natural bone minerals. When implanted, bone can easily integrate into the matrix and bonds with HA quickly. PVA being a bioinert material does not support proper bone integration on its own; the reinforcement of nHA can aid the bone to integrate with the PVA matrix. In vitro bioactivity evaluation can study the response of these composite scaffolds on subjecting to microenvironment application by examining the apatite-forming ability in SBF. SEM micrographs were taken to confirm the apatite formation of the scaffolds (Figure 6). The SEM result has shown an enhanced bioactivity of PHA composite scaffolds than PVA. The reinforcement of nHA in the PVA matrix has enhanced the apatite formation, as PVA alone does not support it [26]. It has been reported that an increase in crystallinity also increases the apatite formation. XRD data have shown an increase in crystallinity with the increase in the concentration of nHA as evidenced by Wu and Xiao [27]. The micrograph of PHA 3 composite scaffold showed dense and homogeneous apatite formation when immersed in SBF. This is due to the proper dispersion of nHA in the PVA matrix leading to this apatite growth in SBF. From the SEM micrographs of PHA 4 and PHA 5 (Figure 6), apatite formation was not homogenous compared to PHA 3. This is due to the improper dispersion and agglomeration of nHA in a PVA matrix that has influenced the nonhomogeneous distribution of apatite

when soaked in SBF. These results were also supported by in vitro degradation studies (Section 3.6). Energydispersive spectroscopy was also performed on the apatite formed during immersion in SBF, and its Ca/P ratio was found to be 1.66, which is close to the stoichiometry of the human bone.

3.8 Hemocompatibility test

Blood compatibility is one of the most important properties that have to be tested on the scaffold material, as this scaffold on implant in the microenvironment has to be in contact with body fluids for a long period of time. During this time period, their interaction may lead to cell damage and blood clotting (thrombus). The damage in the membrane of blood cells will release hemoglobin, which in turn induces acute renal failure. Therefore, it is essential to study the interaction of blood components with scaffold material. Hemolysis test was performed to estimate the blood compatibility of the composite scaffolds. The hemocompatibility of scaffold material was estimated by quantifying the amounts of hemoglobin released from erythrocytes in whole blood when comes in contact with scaffolds. The percent hemolysis values of scaffolds are summarized in Table 3. Positive and negative controls have shown 100% and 0% hemolysis,

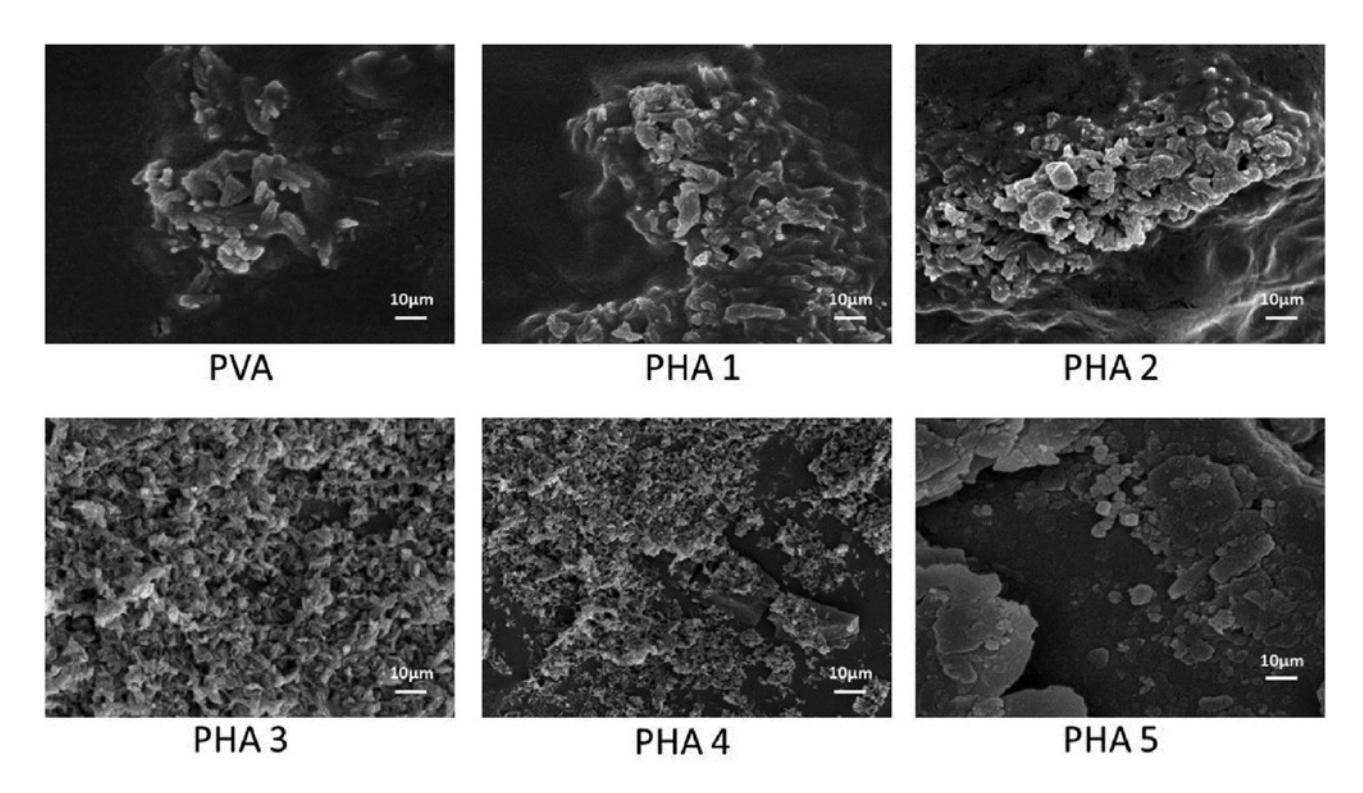


Figure 6: In vitro bioactivity studies of PVA-nHA composites in SBF.

Table 3: Percent hemolysis of PVA-nHA composites.

Samples	Hemolysis (%)
+ve control	100
-ve control	0
PVA	0
PHA 1	0.96
PHA 2	0.26
PHA 3	0.84
PHA 4	2.15
PHA 5	1.19

respectively. The percent hemolysis values varied from 0.26% to 2.15%. All values were <5%, showing the hemocompatible nature of the prepared composite scaffolds. The PVA sample has shown highest hemocompatibility with 0% hemolysis. It can be observed that, with the increase in the amount of nHA above 3% (w/v), hemolysis has increased to 2.15% and 1.19% in PVA 4 and PVA 5 composite scaffolds, respectively. These data revealed that, with the addition of nHA, blood compatibility decreases. This is due to the interaction of ionic groups of nHA with blood, leading to high hemolysis. As observed in the XRD pattern (Figure 2), PHA 4 and PHA 5 samples that were more crystalline and hence with a less distorted structure had a higher hemolysis rate compared to less crystalline (PHA 1, PHA 2, and PHA 3) and semicrystalline PVA [28].

3.9 In vitro cell adhesion and morphology

The ability of the scaffold material to encourage cell adhesion and proliferation is an important factor to determine the potential of scaffold for bone tissue engineering. SEM analysis was performed to evaluate the effect of nHA additions on cell attachment, morphology, and mineral production on PVA and PVA-nHA composite scaffolds. Figure 7 shows the SEM micrographs of the human osteoblast-like MG 63 cells seeded on PVA-nHA scaffolds after 48 h. The growth of the osteoblast cells on all PHA composite scaffolds confirmed the biocompatibility of these scaffolds. The PVA scaffold showed globular-shaped cells attached to its surface. The addition of nHA in the PVA matrix enhanced the cell spreading and cell density on composite scaffolds. This might be due to the higher surface area to volume ratio of nHA that provides more space for cells to adhere and proliferate. Cells formed large groups on the scaffold surfaces. Nodule formation and mineralization were also observed in nHA containing scaffolds (PHA 2 and PHA 3) within 48 h of cell culture.

With a further increase in nHA concentration (PHA 4 and PHA 5), the number of adhered cells and mineralization was decreased. This is due to the combined effect of an increase in the crystallinity and contact angle of PHA 4 and PHA 5.

3.10 In vitro cell viability and proliferation studies

The ability of the scaffold material to promote cell proliferation is an important factor for osseointegration. The PVA-nHA composite scaffolds were tested for cell viability and proliferation in contact with MG 63 cell line for 48 h of culture. The MTT assay results are shown in Figure 8. At 48 h after cell seeding, the PVA-nHA scaffolds showed significantly higher cell proliferation compared to the control (24 well plate). The results showed that the addition of nHA encouraged cell proliferation. This is due to the higher surface area to volume ratio of nHA, which provides more space for cells to proliferate. Cell viability and proliferation increased up to 3% nHA (PHA 3). With a further increase in nHA concentration (PHA 4 and PHA 5), there was a slight decrease in the number of viable cells. This decrease is due to the increase in crystallinity and contact angle of PHA 4 and PHA 5 that might have inhibited the osteoblast cell proliferation [29].

3.11 ALP activity

ALP activity is examined to analyze the bone-forming ability of osteoblast cells cultured on the scaffolds. ALP is the characteristic marker for osteoblast differentiation at an early stage. ALP hydrolyzes pNPP into p-nitrophenol (pNP) and phosphate. Therefore, the ALP activity of the scaffolds can be evaluated from pNP production. Figure 9 shows the relative ALP activity of the scaffolds with the control. As expected, the control showed the least ALP activity compared to the scaffolds. The ALP activity of cells grown on PVA-nHA composite scaffolds was higher than the PVA scaffold. With the addition of nHA, ALP activity increases up to PHA 3, as the HA acts as a chelating agent for the mineralization of osteoblast. There was a slight decrease in ALP activity with a further increase in nHA concentration. This might be due to the less number of adhered cells on higher concentrations of nHA (PHA 4 and PHA 5) as evidenced by cell adhesion and proliferation results.

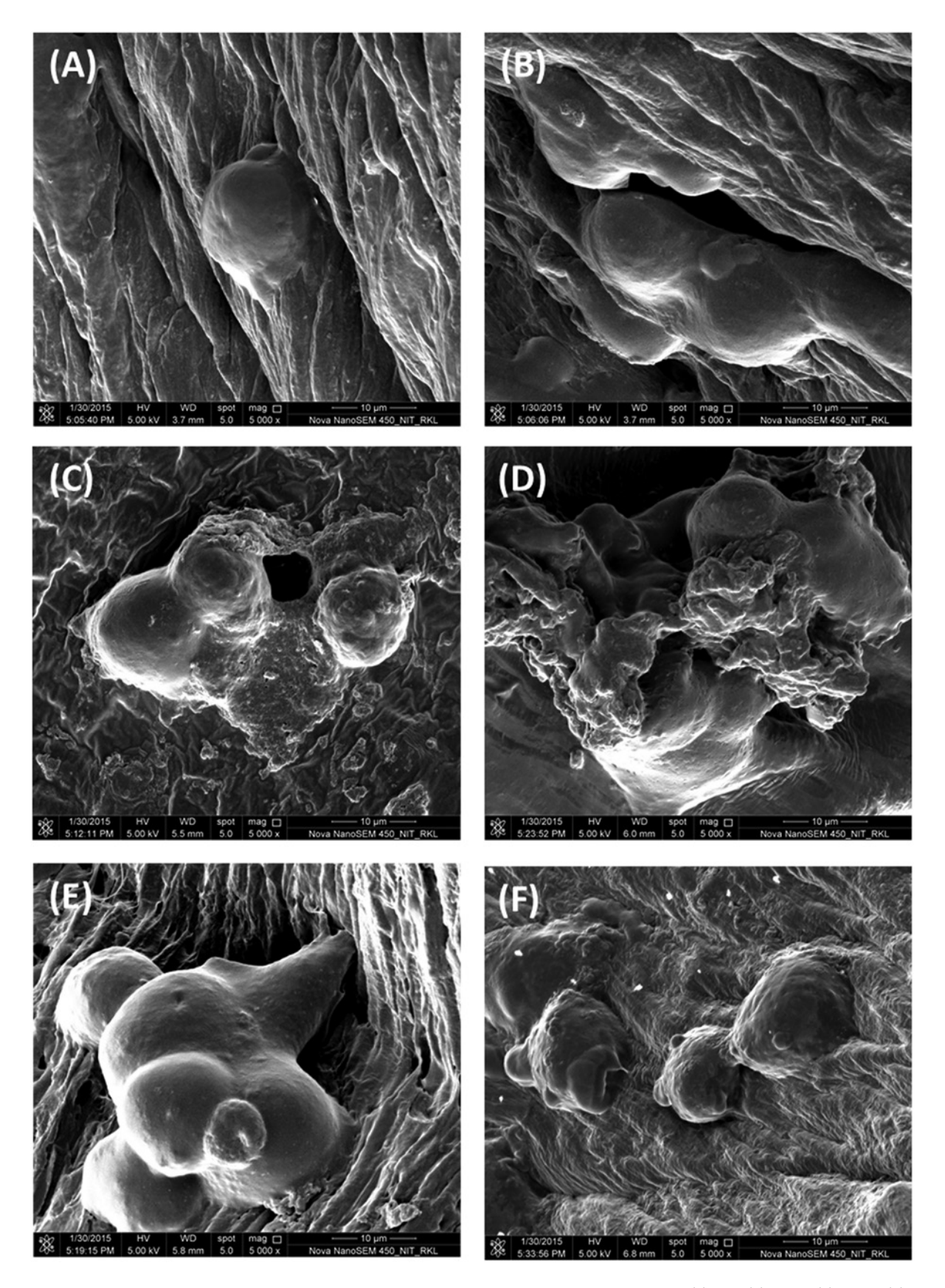


Figure 7: SEM micrographs of PVA and various PVA-nHA composites after MG 63 cell attachment: (A) PVA, (B) PHA 1, (C) PHA 2, (D) PHA 3, (E) PHA 4, and (F) PHA 5.

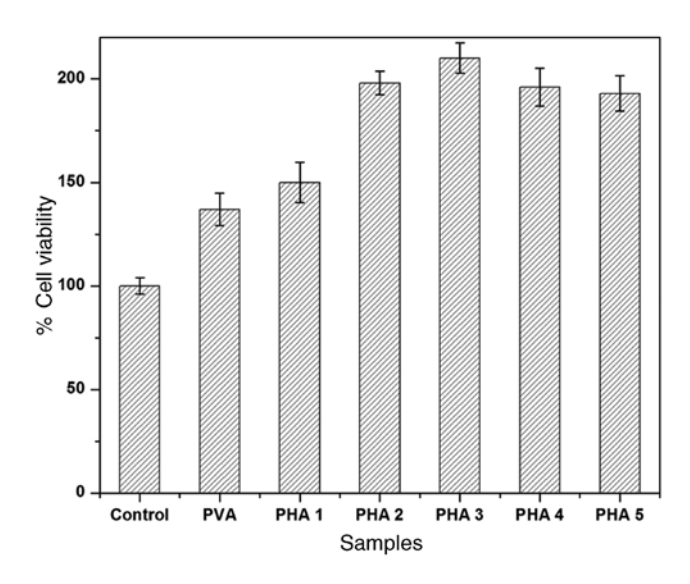


Figure 8: Percentage cell viability of the processed PVA-nHA composites.

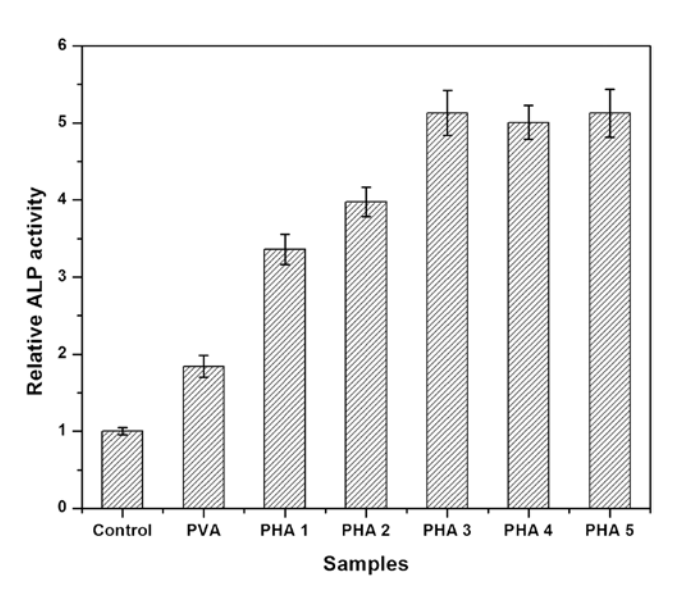


Figure 9: ALP activity of the processed PVA-nHA composites.

3.12 Mineralization assay

Osteoblast-mediated mineralization was confirmed using ARS stain-based assay. ARS binds selectively to calcium salts. Figure 10 shows the ARS staining for mineralization. An increase in the concentration of ARS staining indicated a significant increase in calcium deposition and hence mineralization compared to control. The results are consistent with the SEM and ALP results. The control showed the least mineralization after staining. Mineralization was found to increase with the increase in nHA concentration up to PHA 3 composite scaffolds compared to pure PVA scaffolds. The Ca²⁺ in HA might have contributed to this

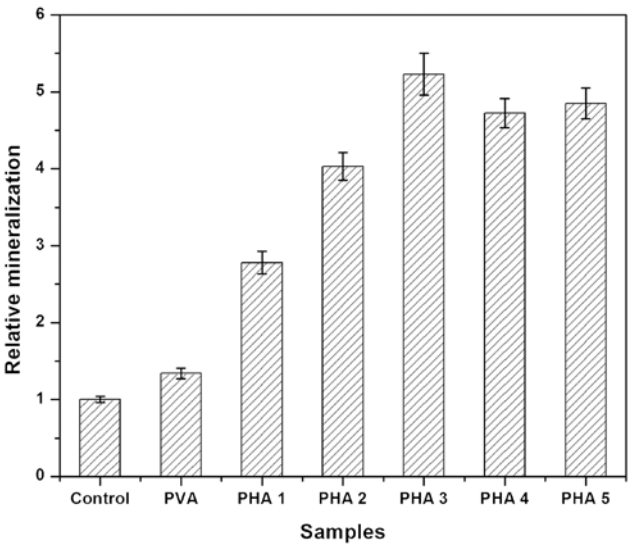


Figure 10: Relative mineralization of the processed PVA-nHA composites.

increase in osteoblast differentiation. PHA 4 and PHA 5 samples showed a slight decrease in ARS staining, indicating a reduction in mineralization. This might be due to the direct contact of agglomerated HA particles with cells causing cell membrane damage *in vitro*. Also, the crystalline nature and increase in hydrophobicity of PHA 4 and PHA 5 decreased the osteogenic differentiation; hence, less mineralization was observed. Cell culture studies for an extended period should be performed to further study the effect of HA on osteoblast cells.

3.13 Mechanical properties

The mechanical properties of the scaffolds were characterized by performing the tensile test, and the values are reported in Table 4. The tensile strength of the composite scaffolds was found to increase initially with the increase in nHA concentration from PVA to PHA 3 (33.5% from PVA to PHA 3 composites). Later, it has been observed that the strength has started to decrease for the PHA 4 and PHA 5

Table 4: Mechanical properties of PVA-nHA composites.

Samples	Tensile strength (MPa)	Young's modulus (GPa)	Elongation (mm)
PVA	23.3±8.6	0.5±0.1	4.2±0.2
PHA 1	24.1±5.9	0.52±0.3	5.5±0.1
PHA 2	24.3±5.9	1±0.8	6.7±0.3
PHA 3	31.1±8.3	1.1±0.8	8.6±0.4
PHA 4	22.1±3.4	1.7±0.4	2.2±0.1
PHA 5	26.1±3.6	1.9±0.4	1.2±0.1

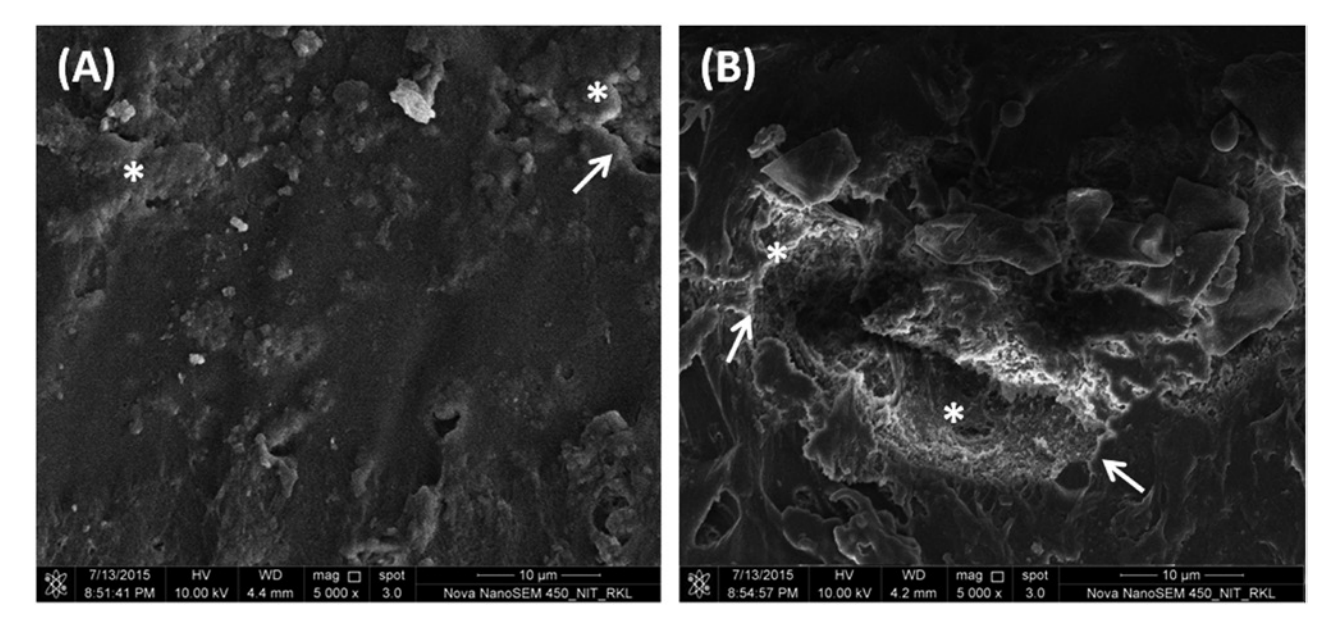


Figure 11: SEM micrographs of fracture surface of (A) PHA 4 and (B) PHA 5. The asterisk represents the agglomeration of nHA particles and the arrow represents the cracks.

composite scaffolds (higher concentration of nHA) with respect to PHA 3. The decrease in tensile strength is due to the agglomeration of nHA in PHA 4 and PHA 5 samples that hinder the effective stress transfer and deteriorates the tensile strength of the composite scaffolds [20]. Further, the addition of nHA has also caused brittleness as evidenced by the less elongation of PHA 4 and PHA 5 scaffolds. The Young's modulus of the composites was found to increase with the increase in nHA concentration. This increase in Young's modulus is due to the improved rigidity of PVA-nHA composites with the addition of nHA, increasing the capability of the scaffolds to resist external forces. As observed in Table 4, the values for elongation at break first increased with the addition of nHA up to 3% and then decreased drastically with the further addition of nHA in PHA 4 and PHA 5. nHA interferes with van der Waals forces and hydrogen bonds between PVA chains, making it more flexible. Also, a strong interfacial adhesion between organic and inorganic phases up to 3% nHA, as reflected in the increase of tensile strength up to PHA 3, could be one of the reasons for the increase in elongation. Therefore, PVA chains elongate without creating cavitations at the interface of the PVA and nHA until PHA 3. The lack of interfacial adhesion in PHA 4 and PHA 5 resulted in an early failure at the interface, leading to weak mechanical properties. The fractured surfaces of the PHA 4 and PHA 5 composites were examined using SEM (Figure 11A and B). The results confirmed the agglomeration of HA in the polymer matrix. This agglomerated HA may have affected the mechanical properties of the PHA 4

and PHA 5 composites. Cracks were also observed in the matrix due to agglomerated particles. The mechanical test results have revealed that the composite scaffolds with 3% (w/v) nHA (PHA 3) have shown the best mechanical properties in comparison with the PHA 4 and PHA 5 composite scaffolds.

4 Conclusion

PVA-nHA composite scaffolds with various concentrations of nHA were developed and characterized in a physiological environment. SEM micrographs revealed the agglomeration of nHA for higher concentrations (4% and 5%, w/v) in PHA 4 and PHA 5 composite scaffolds. The micrograph of PHA 3 composite (3%, w/v) shows even and homogenous distribution of nHA in the PVA matrix. In the XRD analysis, there is no contamination or phase change during the processing of PVA-nHA composites. All composite scaffolds have exhibited a contact angle of <80°, indicating their hydrophilic nature. PHA 3 composite scaffold has shown nominal swelling studies and degradation studies as well as dense and homogenous apatite formation on immersion in SBF for a duration of 4 weeks. On the contrary, the composite scaffolds PHA 4 and PHA 5 have shown nonhomogenous apatite formation on immersion in SBF due to the agglomeration of nHA in the PVA matrix. The percentage hemolysis for all composites was found to be <5%, indicating the high hemocompatible nature of

these composite scaffolds. Osteoblast adhesion, proliferation, ALP activity, and mineralization were significantly higher on composite scaffolds. This was attributed to the enhanced biocompatibility of PVA-nHA composite scaffolds, especially with PHA 2 and PHA 3. PHA 3 also showed the highest tensile strength of 31.1 MPa with an increase in strength of 33.5% compared to PVA scaffolds, whereas PHA 4 and PHA 5 exhibited less strength and undergone brittle failure. Hence, PHA 3 composite scaffold could be the optimum composition of nHA (3%, w/v) among the other composite scaffolds and can be engineered further for bone tissue application. The prepared PVA-nHA composite material shows potential as a substitute for scaffolds for bone tissue engineering and can be developed as an advanced material for bone tissue implants.

Acknowledgments: The authors acknowledge the support provided by the Department of Biotechnology and Medical Engineering, National Institute of Technology, Rourkela, for the successful completion of this research study.

References

- [1] Datta HK, Ng WF, Walker JA, Tuck SP, Varanasi SS. J. Clin. Pathol. 2008, 61, 577-587.
- [2] Nakamura H. J. Hard Tissue Biology. 2007, 16, 15-22.
- [3] Nair LS, Laurencin CT. Prog. Polym. Sci. 2007, 32, 762-798.
- [4] Coombes AGA, Verderio E, Shaw B, Li X, Griffin M, Downes S. Biomaterials 2002, 23, 2113-2118.
- [5] Seal BL, Otero TC, Panitch A. Mater. Sci. Eng. R-Rep. 2001, 34, 147-230.
- [6] Chua CK, Leong KF, Tan KH, Wiria FE, Cheah CM. J. Mater. Sci. Mater. Med. 2004, 15, 1113-1121.
- [7] Asran AS, Henning S, Michler GH. Polymer 2010, 51, 868-876.
- [8] Abdal-hay A, Kim CI, Lim JK. Ceram. Int. 2014, 40, 4995-5000.

- [9] Degirmenbasi N, Kalyon DM, Birinci E. Colloids Surf. B 2006, 48, 42-49.
- [10] Kobayashi H, Kato M, Taguchi T, Ikoma T, Miyashita H, Shimmura S, Tsubota K, Tanaka J. Mater. Sci. Eng. C 2004, 24,
- [11] Poursamar SA, Azami M, Mozafari M. Colloids Surf. B 2011, 84, 310-316.
- [12] Pan Y, Shen Q, Pan C, Wang J. J. Mater. Sci. Technol. 2013, 29,
- [13] Jurczyk M. In Biomaterials for Dental Applications, Jurczyk K, Jurczyk, MU, Eds., Pan Standford Publishing, CRC Press, 2012, n 368.
- [14] Sun JS, Tsuang YH, Liao CJ, Liu HC, Hang YS, Lin FH. J. Biomed. Mater. Res. 1997, 37, 324-334.
- [15] Haroun AA, Gamal-Eldeen A, Harding DR. J. Mater. Sci. Mater. Med. 2009, 20, 2527-2540.
- [16] Kokubo T, Takadama H. Biomaterials 2006, 27, 2907-2915.
- [17] Nie L, Chen D, Suo J, Zou P, Feng S, Yang Q, Yang S, Ye S. Colloids Surf. B. 2012, 100, 169-176.
- [18] Pal K, Pal S. Mater. Manuf. Processes 2006, 21, 325-328.
- [19] Standard test method for tensile properties of polymer matrix composite materials, D3039M-00 (2002), ASTM International, West Conehohoeken, PA 19428-2959.
- [20] Yusong P, Dangsheng X, Xiaolin C. J. Mater Sci. 2007, 42, 5129-5134.
- [21] Pan Y, Xiong D. J. Wuhan Univ. Technol.-Mater. Sci. Ed. 2010, 25, 474-478.
- [22] Bundela H, Bharadwaj V. Polym. Sci. A 2012, 54, 299-309.
- [23] Mollazadeh S, Javadpour J, Khavandi A. Ceram. Int. 2007, 33, 1579-1583.
- [24] Chau TT, Bruckard WJ, Koh PTL, Nguyen AV. Adv. Colloid Interface Sci. 2009, 150, 106-115.
- [25] Schakenraad JM, Lam KH. Tissue Engineering of Vascular Prosthetic Grafts, Landes Bioscience, Austin, 1999.
- [26] Wang X, Li Y, Wei J, Groot K. Biomaterials 2002, 23, 4787-4791.
- [27] Wu C, Xiao Y. Bone and Tissue Regeneration Insights 2009, 2,
- [28] Jadalannagari S, Deshmukh K, Ramanan SR, Kowshik M. Appl. Nanosci. 2014, 4, 133-141.
- [29] Zhu X, Eibl O, Berthold C, Scheideler L, Geis-Gerstorfer J. Nanotechnology 2006, 17, 2711-2721.